Superficies y Vacío ***26(3)*** *79-83, septiembre de 2013*

Crystallization of PNIPAM-hydrogel nanospheres inferred by static light scattering

Reyes-Contreras D.*, [a], Mayorga-Rojas M.
Facultad de Ciencias, Universidad Autónoma del Estado de México
Av. Instituto Literario 100, Colonia Centro, Toluca, Estado México

Rojas-Ochoa L.
Departamento de Física, CINVESTAV-IPN
Av. Instituto Politécnico Nacional 2508, 07360 México D.F., México

Haro-Pérez C.*
Departamento de Ciencias Básicas, UAM-Azcapotzalco
Av. San Pablo 180, 02200 México D.F., México
(Recibido: 10 de octubre de 2012; Aceptado: 30 de julio de 2013)

In this paper we present a kinetic study on crystallization of a colloidal dispersion formed by thermosensitive Poly-N-Isopropylacrylamide (PNIPAM) nanospheres. The liquid-crystal transition is induced by decreasing the temperature of the dispersion and the crystallization process is monitored by measuring the evolution of the static structure factor of the dispersion by means of light scattering techniques. The measured static structure factor confirms the formation of a mesoscopic crystal array at the final equilibrium state, which is preceded by two stages: nucleation and crystal growth.

Keywords: Hydrogel; Light scattering; Crystallization kinetics

1. Introduction

The characterization of colloidal systems is an issue of great importance in basic science and is considered a cutting edge research because they have numerous applications in the chemical industry [1, 2], biological processes [3-5], among others. To cite some examples, we can find colloidal dispersions of biological interest (for instance, blood and protein dispersions) [6-8], of environmental interest (particles dispersed in polluted water or in the atmosphere) [9] or of industrial interest (paints or glues) [10, 11]. Due to colloidal particles can be seen as "giant atoms", colloids are useful model systems for studying structural properties of matter [12, 13] and kinetics of phase transitions such as liquid-crystal transition and glass formation [14]. Any progress in the study and understanding of colloidal phase transitions could be useful for describing globular protein and DNA crystallization [13], since understanding of these processes requires knowledge of the dynamics and structural behavior that lead to the formation of these phases [15].

Colloidal suspension behavior can be modulated experimentally either by changing the surface properties of colloidal particles by chemical methods or modifying the solvent properties as, for example, the ionic strength [16-18]. From a theoretical and computational point of view, this can be controlled by modulating the interaction potential and the solvent properties [19, 20]. The most important parameters in the study of the structure of a colloidal system and thus, the phase behavior, are particle density, temperature and interaction potential among particles. In general, the latter may be completely related to particle density and contains the particle characteristics (soft, hard, core-shell structure, among others) [14, 19, 20].

In this work, we study the liquid-crystal transition of temperature-sensitive hydrogel suspensions. The election of this system obeys to the intrinsic interest of these particles and to the simplicity to control its phase behavior by changing temperature, since these particles vary their size, and consequently, their volume when a change in temperature occurs [21-23]. In particular, our aqueous hydrogel dispersion is formed by Poly-N-Isopropylacrylamide (PNIPAM) nanospheres, which have been extensively studied due to their very interesting properties and applications [22, 24-27]. Hydrogel particles consist of randomly cross-linked polymer chains with water filling the interstitial spaces of the network. PNIPAM nanospheres systems display a strong temperature dependence of particle volume, exhibiting a volume phase transition at a critical temperature close to 34 ºC [22, 25-28]. Above the critical temperature, polymeric chains are hydrophobic and expel the water, so that the particle volume diminishes (*condensed phase*), below this temperature polymer chains are hydrophilic so water can diffuse into the polymeric network increasing the volume of the particle (*expanded phase*) [22, 29-30]. The dependence of the particle volume on temperature makes these particles ideal candidates for being used as drug delivery systems [31-33]. Moreover, hydrogels have been used to encapsulate fluorescent nanoparticles to inhibit their toxicity and may be used in bioimaging applications [23, 29].

In this paper, we perform a kinetic study of the liquid to crystal transition of an aqueous solution of charged Poly-N-Isopropylacrylamide nanospheres when the temperature

* dreyes.fc@gmail.com , cehp@correo.azc.uam.mx
[a] Ph. D. Student, Universidad Autónoma del Estado de México.

is changed from 45 ºC to 30 ºC. At the initial temperature, 45 ºC, the particles are in their collapsed state and the sample shows a liquid like structure, typical of charged colloidal particles. After quenching to 30 ºC, the system crystallizes in a body-centered-cubic lattice (BCC). Crystallization kinetics is investigated by means of light scattering technique by obtaining the crystallinity factor from the analysis of the main peak of the static structure factor $S(q)$.

2. Experimental Procedure

The hydrogel nanospheres under study are composed of Poly-(N)-Isopropylacrylamide (PNIPAM) and they were synthesized by the emulsion-polymerization method under the presence of surfactant (sodium dodecylsulfate) in an inert atmosphere of nitrogen [34]. The resulting particles are electrostatically stabilized due to the use of potassium persulfate as initiator of the reaction, so that the obtained dispersion is stable at temperatures above its critical temperature (34 ºC). The elasticity of the particles is controlled by the amount of crosslinker used in the synthesis which, in our case, is methylene bisacrylamide. After synthesis, the sample is dialyzed and then centrifuged in order to remove the surfactant and the residual monomer. Finally, the system is diluted with ultrapure water to the desired concentration and deionized by addition of ion exchange resins in quartz cells tightly sealed. At the concentration under study, our system undergoes a transition from liquid to crystal as a function of temperature. To study the evolution of the sample during crystallization, the dispersion is first equilibrated at 45 ºC (where the sample shows a liquid like structure) and then quenched by immersing the sample in a thermostat bath to the desired temperature of 30 ºC (where the sample crystallizes in a *bcc* lattice). Once the sample reaches thermal equilibrium, around 10 minutes after quenching, the crystallization process was monitored by measuring the time evolution of the static structure factor *S(q)* from its initial state after quenching until its final equilibrium state. The structure was obtained by using a light scattering device 3D-DLS (*LS Instruments AG, Friburg Switzerland*) which operates with a He-Ne laser as a light source that emits at a wavelength of 632.8 nm. The sample cell is placed in the center of a decaline vat, which is in contact with a bath whose temperature is controlled by a thermostat. The light scattered by the sample is detected with two avalanche photodiodes (APD) and the output signals are fed into a digital multitau correlator (FLEX) that calculates the intensity cross-correlation function. We should point out that this device allows us to measure the single scattered light in the presence of multiple scattering. The structure factor is measured in the angle interval that goes from 20 ° to 150 °.

3. Results and Discussion

As it was mentioned previously, our system undergoes a liquid-crystal transition as a function of temperature that can also be detected by visual assessment. Crystallization can be observed when temperature is decreased below a certain value by the naked eye, from the iridescence the crystallized sample displays under illumination with white light. In order to characterize this transition, we perform light scattering experiments to evaluate *S(q)* that accounts for the structure of the suspension. The averaged structure factor can be extracted directly from scattered light intensities by means of $S(q) = [\rho_0 I(q)]/[\rho I_0(q)]$, where $I_0(q)$ is the light intensity scattered by a sample of non-interacting particles with number density ρ_0 and $I(q)$ is the light intensity scattered by the correlated sample of number density ρ. Interested readers in light scattering can read references [35-37] for more details in the experimental technique**.** For temperatures over 33 ºC approximately, the system exhibits a static structure factor that is typical of a fluid, as we can observe in Figure 1, where we show the experimental structure factor $S(q)$ of our PNIPAM colloidal solution at 36 ºC. The *S(q)* consists of a main peak followed by successive damped oscillations that decay to 1 for scattering vectors much larger than the q-value corresponding to the main peak (0.0094 nm^{-1}). Additionally, the height of the main peak is lower than 2.8, confirming the existence of a liquid state according to the Hansen-Verlet criterion [38], which is a structural criterion used to establish the liquid-solid transition from the height of the mean peak of *S(q)*.

In order to obtain a more detailed analysis of the experimental structure factor in the liquid state, we have solved the Ornstein-Zernike equation with the Hypernetted Chain closure relation by assuming a repulsive Yukawa potential [39]. The result is plotted in the Figure 1 as a solid line and the agreement found between experiment and theory confirms the existence of a liquid-like order in our PNIPAM suspension and the long range nature of the electrostatic repulsive interaction among our microgel particles.

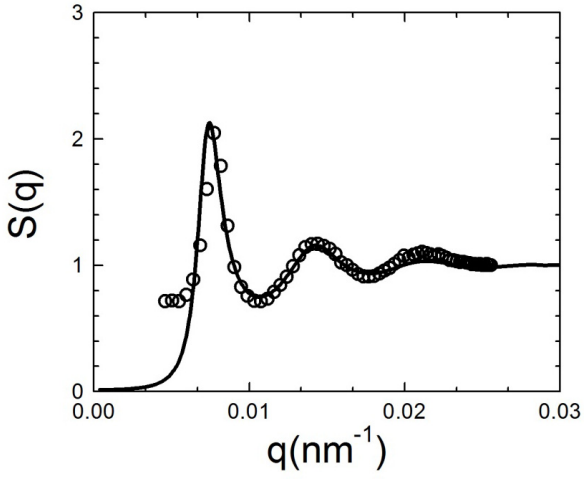

Figure 1. Static structure factor of a PNIPAM colloidal system measured at 36 ºC (symbols) and its corresponding fit obtained by using integral equations theory [39] and assuming a purely repulsive Yukawa potential.

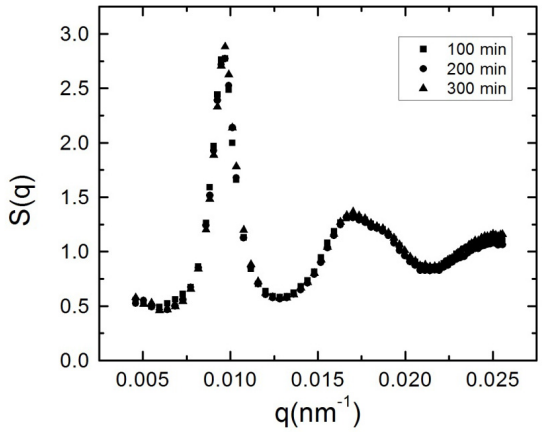

Figure 2. Measured $S(q)$ of PNIPAM dispersion during the first 300 minutes after quenching at 30 ºC.

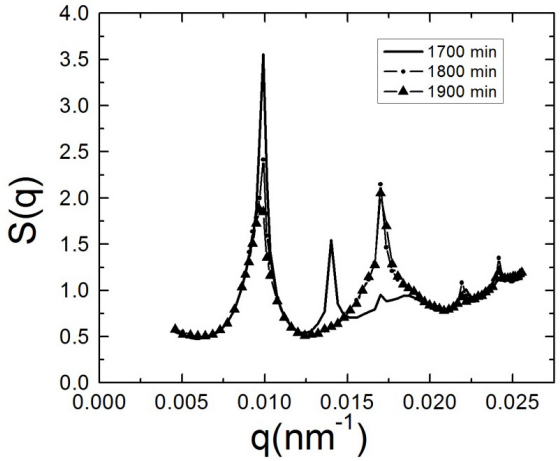

Figure 3. Measured *S(q)* for the PNIPAM sample obtained 1700 minutes (solid line), 1800 minutes (circles) and 1900 minutes (triangles) after quenching at 30 ºC.

Once the liquid state has been described, we look into the evolution of the liquid-crystal phase transition that takes place when the system is cooled down to 30 ºC. The evolution of the static structure factor was measured from their initial liquid state, immediately after quenching at 30 ºC, until the system reaches its final equilibrium state. In figure 2 we present the structure factors measured during the first 300 minutes after quenching. As we can observe, the initial structure of the dispersion at 30 ºC is very similar to that presented in Figure 1, what implies that the system is still in the liquid phase. However, we can appreciate a slight difference comparing with Figure 1, which is the appearance of a small shoulder placed at the right of the maximum of the second peak. In the literature, this shoulder has been associated to the existence of crystalline precursors in the sample [19] and is a hallmark of future crystallization of the system.

During time the structure evolves notably. As an example, we show in figure 3 the static structure factors measured 1700 minutes, 1800 minutes and 1900 minutes after quenching. In this figure we observe that the main and second peaks become narrower and the structure shows the presence of Bragg peaks, which are typical of crystalline phases. These results provide clear evidence of the evolution of our system to a crystal phase but, at this time, it is not possible to say something about the final crystalline arrangement that the system will reach. The evolution of the system structure is recorded until we do not observe any changes. This occurs after 7000 minutes as shown in Figure 4, where we can see that the last three measured static structure factors, measured 8600 minutes, 8700 minutes and 8800 minutes after quenching, display the same Bragg's peaks at the same wave vectors and have almost the same height.

The presence of Bragg peaks confirms that the equilibrium state of the hydrogel dispersion is the crystalline phase. By taking into account the analogy between colloidal crystals and their atomic or molecular counterparts, one can perform crystallographic analysis of the static structure factor and identify in which lattice our dispersion crystallizes. By analyzing the relative positions of the Bragg peaks that appear in $S(q)$ we identify their corresponding Miller indexes (hkl), which are indicated in Figure 4 and correspond to a body centered cubic structure (BCC). The lattice constant "a" has a value of 920 nm and can be estimated by applying$q_{hkl} = 2\pi a^{-1}\sqrt{h^2 + k^2 + l^2}$, where q_{hkl} are the wavevectors that correspond to the peak positions of the static structure factor [23]. We should note that the hydrogel radius increases from 73 nm to 143 nm when the temperatures diminishes from 45 ºC to 30, what implies that the volume fractions is increased by a factor of approximately 8 whereas the particle number density is kept constant.

A fundamental characteristic of colloidal systems is the Brownian motion that their particles undergo due to interactions with solvent molecules. It is well known that increasing the volume fraction of colloidal particles, their Brownian dynamics is altered by the effect of hydrodynamic forces, which are transmitted through the solvent, and direct interactions present among particles [19, 20]. The aforementioned increase of the volume fraction of our system that occurs when the temperature decreases from 45 ºC to 30 ºC leads to a diminution of the separation distance between the particle surfaces and, consequently, to a change in the existing interparticle interaction.

The evolution of the system to a crystalline state is associated with the fact that the system tends to evolve until it reaches its equilibrium state, which implies that the PNIPAM nanospheres explore all the possible configurations to find the optimal configuration that minimize the energy of the overall system.

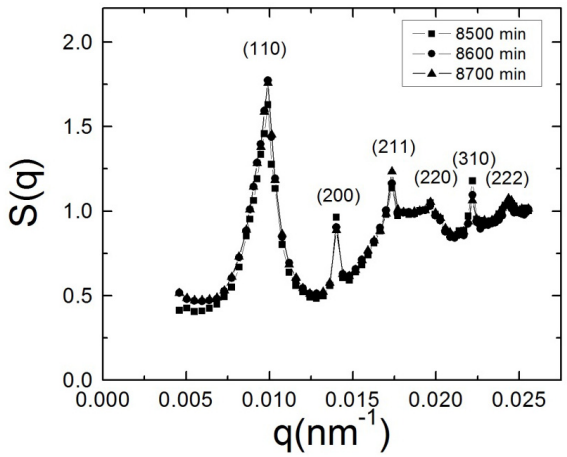

Figure 4. Measured *S(q)* for the PNIPAM colloidal solution. The peak positions correspond to (110), (200), (211), (220), (310) and (222) reflections of a BCC structure.

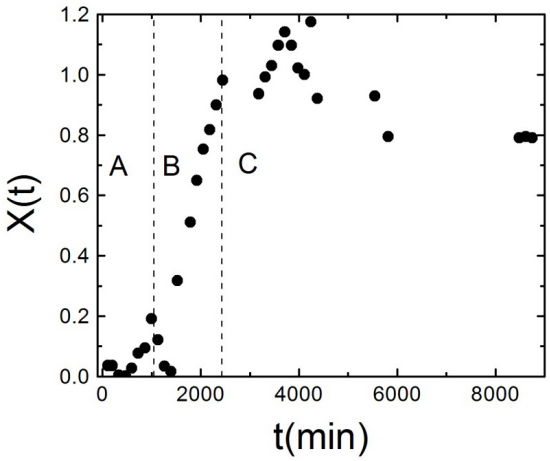

Figure 5. Crystallinity behavior of hydrogel colloidal system at 30 ºC.

In order to describe the evolution of the system during crystallization, we calculate the degree of crystallization of the sample, $X(t)$ from the main peak of the static structure factor by using $X(t) = c\int_{\Delta q} S_c(q,t)dq$, where Δq is the width of the main peak of the static structure factor at half maximum, c is a normalization constant, and $S_c(q,t)$ is the structure factor of the crystalline phase at time t after quenching [40-43]. $S_c(q,t)$ is obtained by subtracting the background fluid structure, that is the initial measured structure factor *S(q, t=0)* to the structure factor measured at time t that corresponds to the overall system (fluid and crystalline phase) *S(q,t)*, $S_c(q,t) = S(q,t) - S(q,t=0)$ [24, 35-37]. The fraction of the sample that is in the crystal phase $X(t)$ shows an abrupt increase as can be seen in Figure 5. Initially, for times lower than 1700 minutes $X(t)$ shows a small increase, afterwards we find the aforementioned sharp increase and finally it fluctuates around one. In this way, we can identify three stages in the fluid to crystal conversion: nucleation, growth and final stage labeled in Figure 5 as A, B and C regions respectively. In the nucleation stage (A), the crystalline precursors serve as nucleation centers that lead to the system to the crystallization process. The growth stage (B) corresponds to a sharply increase of the crystal phase, where the nucleation centers grow to form real crystallites which merge to form bigger crystals. In the final stage (C), the particles in the fluid phase diffuse across the solvent until they are attached onto the surface of the big crystal. During the final stage, the hydrogel nanospheres can return to the fluid phase but, in average, the fraction of crystal phase is conserved.

4. Conclusions

In this work, inducing by contact with a heat bath a cooling in an ionic microgel particle suspension, we observe a liquid-crystal transition by light scattering techniques. The final structure of the suspension corresponds to a BCC lattice whose lattice parameter is several times the particle diameter, meaning that the crystal phase appears at very low volume fractions. The small density of the observed crystal is due to the long range of the repulsive interaction potential among particles caused by the presence of electrostatic charges on the particle surface and the low screening that exists at deionized conditions. The kinetic of the fluid-crystal conversion is followed by calculating the fraction of crystal in the sample which allows us to identify different stages in the crystal formation: nucleation, growth and coarsening. In a future work, we are interested in establishing a theoretical model to describe the crystallization process.

Acknowledgements

D. R. C. acknowledges to UAEM for a graduate student scholarship and M. M. acknowledges to CONACyT for the grant 133229. Moreover, C. H. P. thanks PROMEP (Project 22311009) and CONACyT (Project 166645) for financial support.

References

[1] I. Roland, G. Piel, L. Delattre, B. Evrard, Int. J. Pharm. **263**, 85 (2003).
[2] W. Umbach, Progr. Colloid Polym. Sci. **16**, 111 (1998).
[3] D. Wirtz, Annu. Rev. Biophys. **38**, 301 (2009).
[4] N. Nijenhuis, D. Mizuno, J. A. Spaan, C. F. Schmidt, J. R. Soc. Interface **73**, 1733 (2012).
[5] W. C. Ruder, C.-P. D. Hsu, B. D. Edelman Jr., R. Schwartz, P. R. LeDuc, App. Phys. Lett. **101**, 063701 (2012)
[6] S. Martins, B. Sarmento, D. C. Ferreira, E. B Souto, Int. J. Nanomedicine **2**, 595 (2007).
[7] R. Mezzenga, P. Fischer, Rep. Prog. Phys. **76**, 1 (2013)
[8] J. P. K. Doye, A. A. Louis, I. C. Lin, L. R. Allen, E. G. Noya, A. W. Wilber, H. C. Kok, R. Lyus, Phys. Chem. Chem. Phys. **9**, 2197 (2007).
[9] R. Kretzschmar, T. Schäfer, Elements **1**, 205 (2005).
[10] S. Gourianova, N. Willenbacher, M. Kutschera, Langmuir E **40**, 0501379 (2005).
[11] D. Marksteiner, S. Wasser, W. Schartl, Langmuir **25**, 12843 (2009).
[12] P. G. Vekilov, Cryst. Growth Des. **4,** 671 (2004).

[13] J. F. Lutsko, G. Nicolis, Phys. Rev. Lett. **96**, 046102 (2006)
[14] V. J. Anderson, H. N. W. Lekkerkerker, Nature **416**, 811 (2002).
[15] L. F. Filobelo, O. Galkin, P.G. Vekilov, J. Chem. Phys. **123**, 014904 (2005).
[16] C. Haro-Pérez, L. F. Rojas-Ochoa, V. Trappe, R. Castañeda-Priego, J. Estelrich, M. Quesada-Pérez, J. Callejas-Fernández, and R. Hidalgo-Álvarez, "Structural and Functional Properties of colloidal systems" CRC Press, Taylor and Francis Group, ISBN: 978-1-4200-8446-7, Vol. 146, 77-91 (2009).
[17] M. Q. Pérez, A. M. Molina, F. G. González, R. H. Álvarez, Mol. Phys. **18**, 3029 (2002).
[18] M. A. Bevan, J. A. Lewis, P. V. Braun, P. Wiltzius, Langmuir **20**, 7045 (2004).
[19] M. Mayorga, D. O. González, L. R. Salazar, I. S. Holek, J.M. Rubi, Physica A **388**, 1973 (2009).
[20] D. Frenkel, Nature Mater. **5**, 85 (2006).
[21] S. G. Mitra, T. Cai, D. Diercks, Z. Hu, J. Roberts, J. Dahiya, N. Mills, D. Hynds and S. Ghosh, Polymers **3**, 1243 (2011).
[22] I. Galaev, B. Mattiason, Smart Polymers: Applications in Biotechnology and Biomedicine, Taylor & Francis Group, 247 LLC, (USA, 2008).
[23] A. Neogi, H. Everitt, H. Morkoç, T. Kuroda, A. Tackeuchi; IEEE Transactions on Nanotechnology **2**, 1 (2003).
[24] T. Hellweg, C. D. Dewhurst, E. Brükner, K. Kratz, W. Eimer, Colloidal Polym. Sci. **278**, 972 (2000).
[25] B. W. Garner, T. Cai, S. Ghosh, Z. Hu, A. Neogi, Appl. Phys. Express **2**, 057001 (2009).
[26] H. Gao, W. Yang, K. Min, L. Zha, C. Wang, S. Fu, Polymer **46**, 1087 (2005).
[27] B. Y. Zhang, W. D. He, L. Y. Li, X. L. S., W. T. L., K. R. Zhang, J. Polym. Sci. Part A: Polym. Chem **48**, 3604 (2010).
[28] S. Tang., Z. Hu, Z. Cheng, J. Wu, Langmuir **20**, 8858 (2004).
[29] B. W. Garner, T. Cai, Z. Hu, M. Kim, A. Neogi, Applied Physics Express **2**, 075001 (2009).
[30] S. G. Mitra, T. Cai, S. Ghosh, A. Neogi, Z. Hu, N. Mills, Mater. Res. Soc. Symp. Proc. **1064**, 6 (2008).
[31] T. R. Hoare, D. S. Kohane, Polymer **49**, 1993 (2008).
[32] S. Amin, S. Rajabnezhad, K. Kohli, Sci. Res. Essays **3**, 1175 (2009).
[33] S. Giray, T. Bal, A. M. Kartal, S. Kızılel, C. Erkey, J. Biomed. Mater. Res. A. **100**, 1307 (2012).
[34] M. Heskins and J.E. Guillet, J Macromol. Sci. Phys. **2**, 1441 (1968).
[35] J. G. H. Joosten, J. L. McCarthy, P. N. Pusey, Macromolecules **24**, 6690 (1991).
[36] C. Urban, P. Schurtenberger, J. Colloid Interface Sci. **207**, 150 (1998).
[37] J. Berne, Bruce, Pecora Robert, Dynamic Light Scattering with applications to chemistry, biology and Physics, Dover Publications, (Canada, 2000).
[38] J. P. Hansen, L. Verlet, Phys. Rev. **184**, 151 (1969).
[39] G. Nägele, Phys. Reports **272**, 215 (1996).
[40] J. L. Harland, W. van Megen, Phys. Rev. E **55**, 3054 (1997).
[41] W. van Megen, S. M. Underwood, J. Chem. Phys. **88**, 7841 (1988).
[42] S. Tang, Z. Hu, Z. Cheng, J. Wu, Langmuir **20**, 8858 (2004).
[43] S. Iacopini, T. Palberg, Hans J. Schöpe, J. Chem. Phys. **130**, 084502 (2009).